ponentially with atmospheric pressure through the clouds to 10^{-6} above 57 km.

For T_E = 240 K, surface temperatures greater than 700 K are obtained even for our lowest opacity values. Lowering T_E to 230 K drops the surface temperature to as low as 675 K, but slight increases in cloud opacity or water mixing ratio easily bring it up to the measured value. The large cloud particles must have substantial opacity ($\gtrsim$ 0.25 times their opacity at 0.6 μm) in the window regions of the gas mixture for these high surface temperatures to be obtained.

The transition from radiative to convective equilibrium occurs in the middle cloud (50 to 57 km). For the low opacity case only the lower cloud is convective, and for high opacity both the middle and lower clouds can be convective. If the water abundance is low enough below the cloud bottoms, the CO_2 window regions create a subadiabatic layer beneath the clouds. The extent of this layer depends strongly on the water mixing ratio and for a value of 2×10^{-4} it extends to near 35 km before the atmosphere becomes opaque enough to become unstable again. It is interesting to note that Seiff *et al.* (*9*) find evidence for a subadiabatic region in this portion of the measured temperature profile.

If the large cloud particles have infrared-to-visible opacity ratios as large as 0.25, as Boese *et al.* (*10*) report, we conclude that it is relatively easy to obtain the measured high surface temperatures for reasonable water mixing ratios and a globally averaged net flux profile based on the LSFR data. For these cloud opacity ratios, there is always a convective region within the lower cloud deck. A subadiabatic region is also probable, but depends strongly on the exact water abundance and cloud opacity used in the model. Comparison of the measured temperature profile of Seiff *et al.* (*9*) suggests that our cloud bottom temperatures are generally on the low side if one accepts a cloud opacity ratio of 0.25. Increasing the net flux profile to the limit of the probable error bar, an increase of some 35 percent at this altitude, brings the profiles into better agreement.

MARTIN G. TOMASKO
LYN R. DOOSE, PETER H. SMITH
Lunar and Planetary Laboratory and *Optical Sciences Center, University of Arizona, Tucson 85721*

References and Notes

1. M. G. Tomasko, L. R. Doose, J. Palmer, A. Holmes, W. Wolfe, N. D. Castillo, P. H. Smith, *Science* **203**, 795 (1979).
2. R. G. Knollenberg and D. M. Hunten, *ibid.*, p. 792.
3. J. E. Hansen, *J. Atmos. Sci.* **28**, 1400 (1971).
4. L. D. Travis, D. L. Coffeen, J. E. Hansen, K. Kawabata, A. A. Lacis, W. A. Lane, S. S. Limaye, P. H. Stone, *Science* **203**, 781 (1979).
5. R. G. Knollenberg and D. M. Hunten, *ibid.* **205**, 70 (1979).
6. A. T. Young, *Icarus* **32**, 1 (1977).
7. At least for sulfur having properties described by the simplified expression in (*6*).
8. J. B. Pollack and R. Young, *J. Atm. Sci.* **32**, 1025 (1975); J. B. Pollack, *Icarus* **10**, 301 (1969); *ibid.*, p. 314.
9. A. Seiff *et al.*, *Science* **203**, 787 (1979).
10. R. W. Boese, J. B. Pollack, P. M. Silvaggio, *ibid.*, p. 797.
11. This size distribution was assumed to apply down to a lower limit of 0.1-μm radius, below which no particles were included.
12. The mode 1 particles in this region of the upper cloud have a gas-to-particle scale height ratio of 2. All other regions and modes are assumed to be uniformly mixed.
13. It gives us pleasure to acknowledge the support of N. Castillo and A. Holmes in data processing and instrument calibration.

15 May 1979

Preliminary Results of the Pioneer Venus Small Probe Net Flux Radiometer Experiment

Abstract. *Net radiation measurements in the atmosphere of Venus indicate that the bulk of the atmosphere is radiatively cooling at high latitudes and heating at low latitudes. Similarity of features observed by all three probes indicate planetwide stratification. Flux variations within the clouds provide evidence of significant differences in cloud structure. A feature of unusually large opacity found near 60 kilometers at the north probe site is probably related to the unique circulation regime revealed by ultraviolet and infrared imagery. A stable layer between the cloud bottoms and about 35 kilometers contains several features in the flux profiles probably resulting from large-scale compositional stratifications rather than clouds. In the layer below 35 kilometers unexpectedly large fluxes were observed.*

A small probe net flux radiometer (SNFR) was flown on the north, day, and night probes of the Pioneer Venus mission, sampling the atmosphere over a wide range of latitudes and longitudes (*1*). All three instruments operated successfully from deployment down to an altitude of 12.5 km (*2*), measuring the total planar net flux density (termed net flux herein) as a function of altitude. Since the divergence of the net flux equals the radiative power input per unit volume, the altitude derivative of the SNFR measurements directly defines the vertical distribution of radiative energy sources and sinks which power the atmospheric circulations. Also embodied in the SNFR data is information about the opacity structure of the atmosphere; the measured flux profiles place constraints on the sources of opacity—the gases and particulates through which radiative transfer takes place. The preliminary results of this experiment are presented here, following a short description of the instrument measurement characteristics.

The SNFR measures the difference between upward and downward fluxes directly by means of an external sensor with a wide field of view deployed beyond the edge of the probe's heat shield. The sensor consists of a thermopile-equipped flux plate protected by a pair of diamond windows. A heater is incorporated to prevent condensation and to minimize errors produced by a sensor thermal lag relative to the atmosphere. A sensor temperature monitor provides data needed to correct for a temperature-dependent responsivity. The radiation field is mechanically chopped by flipping the sensor at a 1-Hz rate, thereby canceling thermal and electrical offsets generated by the environmental extremes experienced in descent. Further instrumentation details can be found in (*3*).

The SNFR flux measurements spectrally integrate radiation in a wide bandpass from ultraviolet to far infrared with nearly uniform weighting at all wavelengths where significant net flux is possible within the atmosphere (Fig. 1). At the north and night probe sites, where solar radiation was absent, the SNFR measured only planetary radiation. The day probe SNFR measured the sum of the net planetary and net solar fluxes. The angular response of the SNFR, when averaged over a complete probe rotation, approaches the cosine response of an ideal flat plate (Fig. 2). The error in the SNFR fluxes due to angular and spectral response defects is estimated to be less than 1 percent on the basis of simulations performed with an infrared radiative transfer model (*4*).

The net flux measurements from all three probes are shown in Fig. 3 with positive values indicating net upward flux. Note that the solar contribution to the day probe net flux makes the total smaller than observed at the other sites. The altitude scale is based on data from the small probe atmospheric structure (SAS) experiment (*5*). To facilitate direct intercomparisons with other experiments, ground receipt time for each probe is shown on inserted scales. All of the data obtained prior to and immedi-

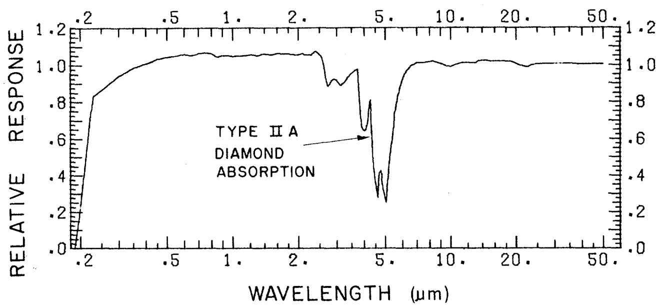

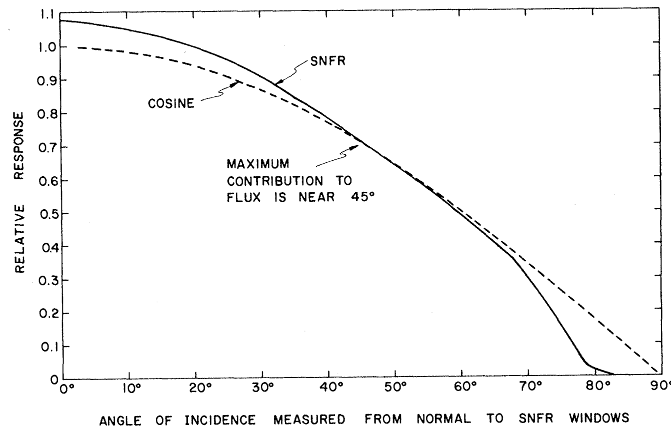

Fig. 1 (left). Relative spectral response obtained with the SNFR. Solar and planetary radiation contributions are weighted nearly equally. The low response near 5 μm is unimportant because of the very high atmospheric opacity in this region. Fig. 2 (right). Relative angular response obtained with the SNFR compared to an ideal flat-plate response.

ately following failure are shown without smoothing. Samples were taken every 4 seconds above approximately 27 km, where the probe bit rate changed, and every 16 seconds below. The suddenness with which the flux measurements went to zero at 12 km indicates that earlier measurements were unaffected, even though the failure of all external radiometers and temperature sensors on all probes near 634 K atmospheric temperature has not been satisfactorily explained. The large regions of extremely smooth data in the profiles give confidence that the instrument was performing properly. The short time scale variability observed in some regions (for example, night probe below 44 km) may be related to probe attitude deviations. Modulations in SNFR flux data can be produced by a nonvertical probe when its spin period differs significantly from the 4-second flux averaging period, an expected condition below 50 km. The relatively small variability observed in the day profile, where the fluxes are small, would be consistent with this explanation if similar buffeting (or inclination) and spin rate were assumed for all probes. Two separate lines of data as shown at 40 km in the night profile could be explained by a tilted probe axis and a probe spin rate near 7.5 rev/min. The shaded regions at the top of each profile indicate an area of uncertainty in the measurements caused by a deployment transient related to rapid changes of the sensor temperature relative to the atmosphere (Fig. 4). Further analysis will probably reduce this uncertainty. Fluxes in the shaded regions have been corrected for changing probe attitude by using flight path angles predicted by NASA. Below the shaded regions the uncertainty of the flux profile should be smaller than the standard deviations of the points shown ($\leq$ 5 W/m^2).

In addition to net flux the external sensor temperature was measured primarily for correcting temperature dependence and for diagnostic use. However, during most of the descent the sensors were so well thermally coupled to the atmosphere that their temperatures are a useful measure of atmospheric temperatures. The results are shown in Fig. 4 as a function of SAS altitude (*5*). They confirm the SAS result that at 60°N the atmosphere is colder between about 60 and 45 km than it is at low latitudes. Failure of the temperature monitor at 634 K occurred very abruptly, as shown, and was essentially simultaneous with the net flux sensor failure. The inset shows the difference between each sensor temperature and the atmospheric temperature as measured by the SAS experiment on the same probe (*5*). The large initial difference of almost 100 K is a result of heating the sensor prior to entry to prevent condensation on the sensor window. The SNFR-SAS temperature difference was within about 5 K from 50 to 12 km. Local adiabats shown in Fig. 4 illustrate the stability of the atmosphere at various levels. Adiabatic lapse rates were calculated according to Staley (*6*), with the use of tables of real gas properties for 100 percent CO_2 (*7*). The region below the clouds from 48 to around 35 km is stable, while regions of very nearly adiabatic lapse rate occur in the lowest cloud layer near 50 km and from about 20 to 30 km.

In an average sense the net flux profiles (Fig. 3) indicate that the bulk of the atmosphere up to about 50 km is radiatively cooling at 60°N and heating at 30°S. This difference in radiative energy transfer could provide a mechanism for driving motions throughout the atmosphere and should be included in future circulation models through composition or cloudiness variations or both. On a finer scale, the flux profiles have significant vertical structure which is most conveniently discussed in terms of the three major atmospheric layers: a cloud layer above altitudes defined by the nephelometer cloud bottoms (*8*); a middle layer between the cloud bottoms and 35 to 37 km within which no backscatter was detected by the nephelometer yet significant structure is evident in the flux profiles; and the bottom layer below 35 km where again no clouds were detected, and where flux divergences vary slowly with altitude. In the clouds major changes in the net flux profiles usually correspond with the three major cloud layers identified by nephelometer backscatter measurements (*9*). In the north and night profiles the lower cloud layer is revealed by regions of relatively depressed fluxes, an indication of relatively increased infrared opacity within the layer. The day probe flux profile shows depressed values in the middle cloud layer but an insignificant effect in the lower cloud which, in this case, appears to have very little vertical thickness and low backscatter (*9*). In the night profile the middle cloud layer stands out as a region of increased net flux relative to the depressed values in the upper and lower clouds, indicating that the infrared opacity of the middle cloud is lower than that of the surrounding clouds. It is clear that nephelometer backscatter and net flux measurements had a relative sensitivity to clouds which varied from region to region. The relative sensitivities provide constraints on the possible constituents of the clouds.

The most unusual feature of SNFR measurements in the cloud layer is evident near 60 km in the north profile, where the backscatter is smaller than at lower altitudes and where the net flux indicates a local source of large opacity. If the opacity increase is indeed due to particles they must have a cross-section ratio of backscatter at 0.9 μm to long-wavelength extinction which is very much lower than that for cloud particles observed at other entry sites. Any of several unusual conditions could account for this situation: the particles are very small, probably less than 0.1 μm in radius; the particles have a very narrow size distribution peaked at a deep minimum in the backscatter cross section; or the particles are nonspherical and preferentially oriented to produce large vertical cross sections (strongly affecting the net flux) and very small horizontal cross sections (making detection difficult for the side-looking nephelometer). Cirrus clouds on Earth, containing hexagonal ice crystal plates, illustrate the conditions suggested by this last possibility. The opacity source might also be gaseous in nature, in which case its absence in the nephelometer traces would be expected. Possible infrared absorbing gases might be H_2O or SO_2, although the mixing ratios needed to produce such a large opacity effect appear to be unreasonably high.

Corroborating evidence for unusual cloud characteristics in the polar cloud cap can be found in Earth-based and Pioneer Venus orbiter infrared radiometer (OIR) data. Prior to the Pioneer encounter, Earth-based infrared imaging of Venus (*10*) identified a sharply defined ring of very low thermal emission relative to the rest of the planet. The feature showed day-to-day variations, sometimes disappearing completely, often varying in latitude. A similar image made within minutes of the probe entries (*11*) indicates that the north probe entered at the edge of a high-latitude thermal feature as cold as any other in the image. This may be related to the feature identified at 75°N by Taylor from OIR data gathered 5 days prior to entry (*12*). Taylor found not only that the temperature measured by the 11-μm channel was unusually low, but also that the 50-μm channel, which normally samples 5 km deeper, measured even lower radiating temperatures. This suggests either water vapor absorption above the 11-μm cloud top, or cloud particles that have greater opacity at 50 μm than they do at 11 μm, a condition not seen in clouds covering the rest of the planet.

The layer below the clouds might be called the stable layer because the lapse rates are subadiabatic throughout (Fig. 4). As in the cloud layer, evidence for stratification is apparent in the flux profiles (Fig. 3). Alternating layers of heating (negative slope) and cooling can be identified in each net flux profile, with heating occurring roughly between 36 and 40 km and again between 45 and 47 km. The existence of corresponding layers in each profile suggests that the structure may be characteristic of midlatitudes (30° to 60°). Again the net flux structure must be caused by mechanisms yielding little 0.9-μm backscatter; very small particles or gases seem likely in this region.

Several surprising SNFR results appear in the bottom layer, where specific expectations based on radiative transfer modeling (*13*) are contradicted by the SNFR flux data. For example, between 12.5 and 35 km the north probe shows radiative cooling at a rate much lower than expected, the rate decreasing with altitude, in contrast to the expected increase. In addition, the north probe flux at 13 km is nearly 60 W/m^2, several times what the model predicts even with as little as 0.01 percent H_2O. The north probe flux data thus indicate that the lower atmosphere has less opacity (is perhaps drier) than expected. The shape of the night profile in this region is simi-

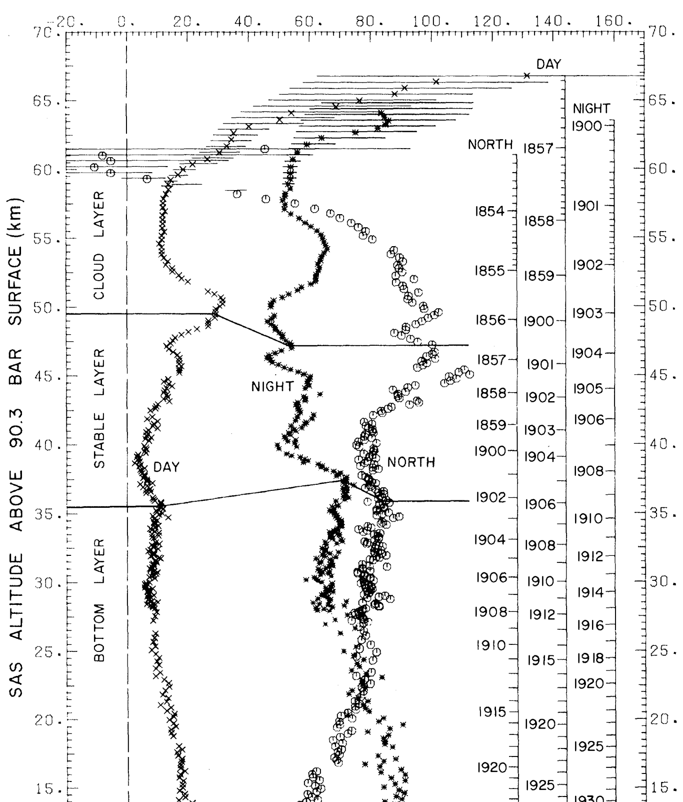

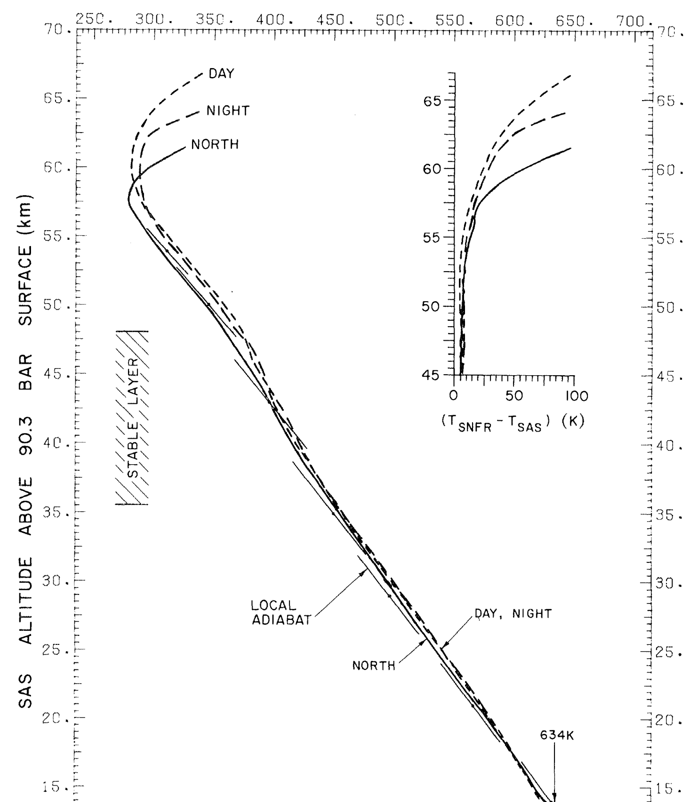

Fig. 3 (left). Net flux density profiles for each small probe. The day, night, and north probes entered at 31.3°S, 28.7°S, and 59.3°N latitude, respectively, and the solar zenith angle for the day probe was 79.9°. Inserted scales are ground receipt times for each probe. The line separating the cloud layer from the stable layer follows nephelometer cloud bottoms. Shaded regions indicate uncertainties resulting from deployment transients. Fig. 4 (right). SNFR sensor temperature profiles for each small probe. The inset shows the deviation of each sensor profile from atmospheric temperature. External sensor failure is apparent from the sudden divergence of the measurements below 13 km.

lar to the north profile except below 27 km, where it begins to deviate with an indication of heating. The start of this deviation is simultaneous with the inception of off-scale readings in auxiliary SNFR voltage-offset data. Although no direct evidence of corresponding flux channel degradation has been found, the offset behavior suggests caution in interpreting the night probe data below this altitude until spare instrument performance tests under similar conditions can be completed.

The day probe profile indicates heating below 27 km, presumably because of solar energy deposition. If the solar net flux below the clouds can be estimated even crudely by differencing the day and night (or north) profiles, it is about four times larger than that expected from large probe solar flux measurements (*14*) after solar zenith angle adjustments. Aside from small effects caused by spectral response differences, this seems to imply significant differences in the clouds at the day and large probe sites above about 60 km.

It is likely that the three layers identified have important implications relevant to the general circulation. In the bottom layer, low latitude heating and high latitude cooling, in the absence of other driving forces, could give rise to a slowly overturning cell with meridional motion toward the equator near the surface (*15*, *16*). Although the flux divergences are small, significant mass transport is possible because the temperature profile is nearly adiabatic in this layer. In the cloud layer, strong circulations have already been observed by Mariner 10 (*17*). The different dynamical regime that was found in the polar region is probably reflected in the significantly different cloud structure found there by several Pioneer Venus experiments as discussed earlier. Although the strong heating observed below 60 km in the high latitude clouds coupled with cooling at the top would ordinarily tend to produce local overturning, the strongly subadiabatic lapse rates there suggest that the energy transport is provided instead by circulations on a much larger scale. This is consistent with motions seen in Mariner 10 images as well as the cloud structural features seen in these images and in orbiter data (*12*), which together indicate large-scale vertical motions in the polar cloud cap. In the middle layer the flux variations are most likely the result of compositional stratifications. The stability of this layer and the similarity of structure from probe to probe again suggest a planetary scale circulation probably driven indirectly by other layers.

The picture of the general circulation should become much clearer when a complete set of winds from the DLBI experiment (*16*) is available. The general circulation and its connection to surface heating and the greenhouse effect will be one subject of future investigations. We also plan to investigate the implications of the SNFR measurements for identifying cloud and gaseous constituents.

V. E. SUOMI
L. A. SROMOVSKY
H. E. REVERCOMB
Space and Engineering Center, University of Wisconsin, Madison 53706

References and Notes

1. L. Colin, *Science* **203**, 743 (1979).
2. Below 12.5 km (relative to the 90.3 isobar) all SNFR external sensors on all three small probes experienced a sudden failure of unknown origin, but presumably related to the SAS temperature sensor failures on all four probes (that is, including the large probe) at approximately the same altitude. The Pioneer Project Office is conducting a study headed by L. Polaski of these and other associated anomalies. The SNFR electronics modules continued to produce normal calibration data until the end of probe transmissions.
3. L. Colin and D. Hunten, *Space Sci. Rev.* **20**, 482 (1977).
4. The 16 spectral interval radiative transfer model used in simulations was provided by J. Pollack.
5. A. Seiff, private communication.
6. D. O. Staley, *J. Atmos. Sci.* **27**, 219 (1970).
7. J. C. Hilsenrath *et al.*, *Tables of Thermodynamic and Transport Properties of Air, Argon, Carbon Dioxide, Carbon Monoxide, Hydrogen, Nitrogen, Oxygen and Steam* (Pergamon, New York, 1960).
8. B. Ragent and J. Blamont, *Science* **203**, 790 (1979).
9. B. Ragent, private communication; see also J. Blamont and B. Ragent, *ibid.* **205**, 67 (1979).
10. J. Apt and R. Goody, *J. Geophys. Res.*, in press.
11. ——, *Science* **203**, 785 (1979).
12. F. W. Taylor *et al.*, *ibid.*, p. 779.
13. R. W. Boese, J. B. Pollack, P. M. Silvaggio, *ibid.*, p. 797.
14. M. G. Tomasko, L. R. Doose, J. Palmer, A. Holmes, W. Wolfe, N. D. Castillo, P. H. Smith, *ibid.*, p. 795.
15. Preliminary results of the DLBI experiment (*16*) indicate that the opposite is true, that is, the bottom of the atmosphere appears to have meridional motion toward the pole, suggesting that the lower cell is indirectly driven.
16. DLBI is the acronym for the differential long-baseline interferometry experiment [see C. C. Counselman III, S. A. Gourevitch, R. W. King, G. B. Loviott, *Science* **205**, 85 (1979)].
17. V. E. Suomi, in *The Atmosphere of Venus*, J. Hansen, Ed. (NASA SP-382) (1974), pp. 42–58.
18. We thank the engineering and technical staff of the University of Wisconsin Space Science and Engineering Center for excellent work in developing the SNFR instrument; especially significant contributions were made by E. E. Richards, R. M. Dombroski, R. A. Herbsleb, R. F. Sutton, G. Bucholtz, J. C. Sitzman, S. Burns, M. Shah, D. Ford, D. Otto, T. Wendricks, R. Dedecker, and E. Grindey. We also acknowledge the efforts of C. Hall and his personnel in the Pioneer Project Office; special thanks are due to L. Polaski, R. Twarowski, J. Terhune, and C. Leidich.

15 May 1979

Venus Winds Are Zonal and Retrograde Below the Clouds

Abstract. *Winds in the lower atmosphere of Venus, inferred from three-dimensional radio interferometric tracking of the descents of the Pioneer day and north probes, are predominantly easterly with speeds of about 1 meter per second near the surface, 50 meters per second at the bottom of the clouds, and more than 200 meters per second within the densest, middle cloud layer. Between about 25 and 55 kilometers altitude the average flow was slanted equatorward, with superimposed wavelike motions and alternating layers of high and low shear.*

The Pioneer Venus differential long-baseline interferometry (DLBI) experiment (*1*) was designed to obtain, for the first time, profiles of vector wind velocities as functions of altitude in the lower atmosphere of Venus. Here we report the first results of the experiment, from the tracking of the day probe, which descended about 12° west of the morning terminator at about 30°S latitude, and the north probe, which descended about 35° east of this terminator at about 60°N latitude. So far we have obtained wind profiles only for altitudes below 55 km for the day probe and below about 40 km for the north probe. We expect eventually to extend the profiles for these probes to approximately 65 km altitude and to obtain similar results for the night and sounder probes.

Preliminary results for the day probe, for altitudes up to 49 km, are given in Fig. 1. All three components, locally downward, westward, and northward, of the probe's velocity vector are plotted against altitude relative to the impact point. The probe's vector position relative to this point was estimated as a function of time directly from the earth-based radio observations. Differencing of the estimated positions at ~ 60-second intervals yielded the velocity components shown here. Our results for the altitude and its time derivative, the vertical component of velocity, agree with completely independent determinations (*2*) based on the assumption of hydrostatic equilibrium, the equation of state of the atmospheric gas, and the in situ pressure and temperature measurements, within our estimated uncertainties of about 1 km and 1 to 2 m sec^{-1}, respectively. Since, in our experiment, the vertical component of velocity is unlikely to have been determined correctly unless the horizontal components were correct at a similar

0036-8075/79/0706-0085$00.50/0